International Journal of Innovative Research in Engineering & Management (IJIREM)
ISSN: 2350-0557, Volume-9, Issue-2, April 2022
https://doi.org/10.55524/ijirem.2022.9.2.107
Article ID IJIRP-2306, Pages 667-676
www.ijirem.org

Integration of Renewable Energy Generating Sources with Micro-Grid

Jadapalli Suresh[1], Bolleddu Mohan Kumar[2], Gunji Suresh[3], Gadde Ravi Varma[4], Kunchala Murali[5], Dr. C. Rajalingam[6], AND Dr. R. Shankar[7]

[1,2,3,4,5]Student, Department of Electrical and Electronics Engineering, PACE Institute of Technology and Sciences, Ongole, Andhra Pradesh, India
[6]Assistant Professor, Department of Electrical and Electronics Engineering, PACE Institute of Technology and Sciences, Ongole, Andhra Pradesh, India
[7]Associate Professor, Department of Electrical and Electronics Engineering, PACE Institute of Technology and Sciences, Ongole, Andhra Pradesh, India

ABSTRACT- The management of remote sites' hybrid wind-and-solar energy-powered micro grids. The battery bank is connected to a shared DC bus from the double fed induction generator (DFIG), which is the device used to convert wind energy. The conversion of solar energy takes place in photovoltaic (PV) arrays. On the common DC bus of DFIG, a DC-DC boost converter efficiently consumes solar energy. The line-side converter with drooping characteristics' indirect vector control is used to regulate the voltage and frequency. It slows the overcharging or discharging of the battery by altering the frequency reference dependent on the battery's energy level. You can run this system without using wind energy. Maximum power point tracking (MPPT) is a component of control algorithms for wind and solar systems. In addition to having external power support to charge the battery without the need for additional power, this system is designed for completely automated operation, taking into account all of the actual system conditions. The system's simulation model is created in the MATLAB environment, and the simulation results are presented in a variety of ways. Low battery charge state, imbalanced load, impervious to wind or sunlight, and non-linear. A 3.7kW wound rotor asynchronous machine and a 5kW photovoltaic array simulator are used to execute the system and produce experimental results that confirm the theoretical model and design.

KEYWORDS- Wind energy, DFIG, Vector Control, Power Quality, Micro-grid, Battery Energy Storage System, Renewable Energy System.

I. INTRODUCTION

There the planet contains sizable distant locations where there isn't enough electricity to produce electricity. Although there are numerous substations connected to the grid, you don't require much power. Biomass, wind, and solar energy are the three main categories of renewable energy. Wind and solar energy are more effective than biomass. We rely on solar and wind energy. These sources' low capacity utilization and excellent efficiency are their key features. However, since nature is erratic, we do not always produce energy. The autonomous system won't be able to produce power as a result. You need to use battery storage (BSE) to solve this issue. Power surges and fluctuations can be prevented by operating each power source at its maximum operating point. Numerous authors have suggested autonomous wind and solar energy systems. These systems needed very large system power supplies and power electronics components for just one power source. Both energy sources are combined and coupled with battery energy storage in these. Hybrid vehicles have a natural ally in wind and solar energy. These two resources can be used to create yearly and daily behaviour patterns.

II. MICRO GRID

A hybrid system involves joining two or more renewable energy sources, such as wind, solar, electric cells, and micro turbine generators, in order to produce electricity for nearby loads or to link to a grid or micro grid. A system of energy is created. Photovoltaic systems and wind turbines support substantially higher combined power reliability than single-power generation because of the properties of photovoltaics' and wind energy.

The load needs a sizable battery bank in order to take the majority of the energy from wind and PV arrays. The development and implementation of renewable DC power sources, as well as the advantages of DC loads in industrial, commercial, and residential applications, have recently given the DC power grid a new lease on life. For integration with various distributed generating systems, DC micro grids have been proposed.

However, before connecting to the DC grid, AC power must be converted to DC. The consequences of the fluctuating nature of solar and wind resources are largely mitigated by combining the two renewable resources into the ideal combination, improving the economics and dependability of the operation of the entire system. Modern-day overviews of grid tide and standalone hybrid solar and wind systems are available in a number of configurations.

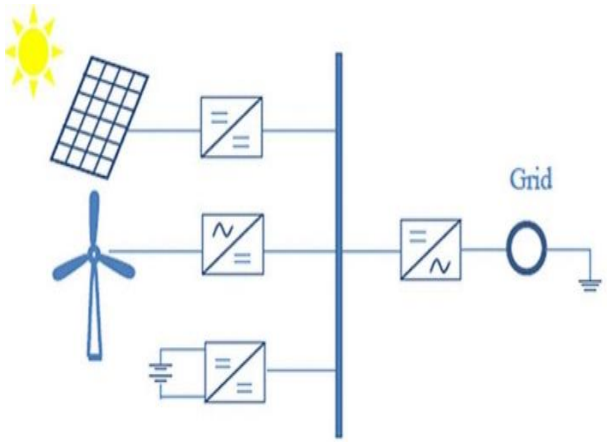

Figure 1: Grid connected hybrid system with DC bus bar

III. SYSTEM MODELING

It was created for areas that needed a maximum of 15kW and an average of 5kW of power. The REGS wind and solar energy blocks are both believed to have a nominal power of 15kW. Both energy blocks are taken into consideration at a 20% utilisation. This will provide the village's whole daily energy needs. According to the schematic, if the wind speed is too low, a 3-pole circuit breaker will be used to disconnect the wind energy source from the grid. Along with the HV side of the solar converter, the DC sides of the RSC and LSC are both connected to the battery bank. The RSC aids in maintaining the wind energy system's rotating speed at the optimum level required by the WMPPT algorithm. The grid's voltage and frequency are under the LSC's control. Ficure displays the system's energy flow diagram.

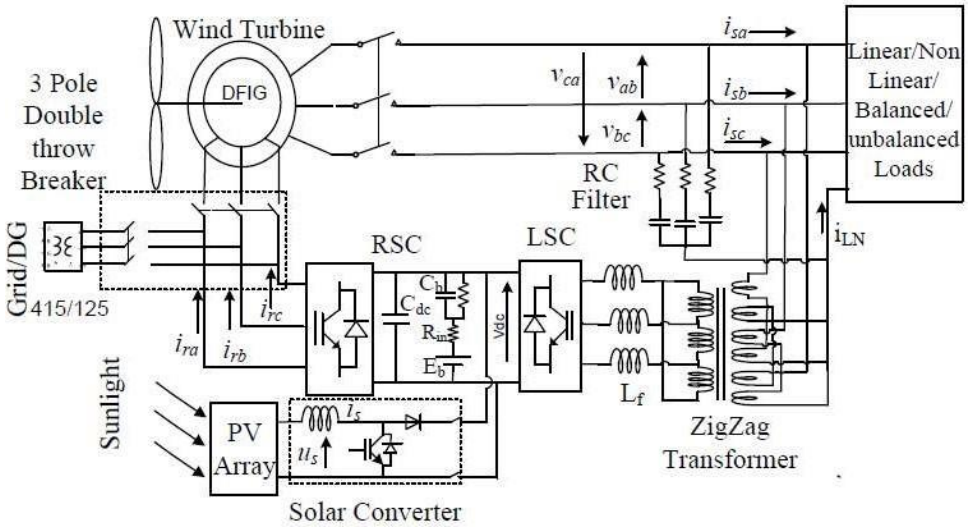

Figure 2: Diagram of a remote micro grid network powered by batteries and using renewable energy sources.

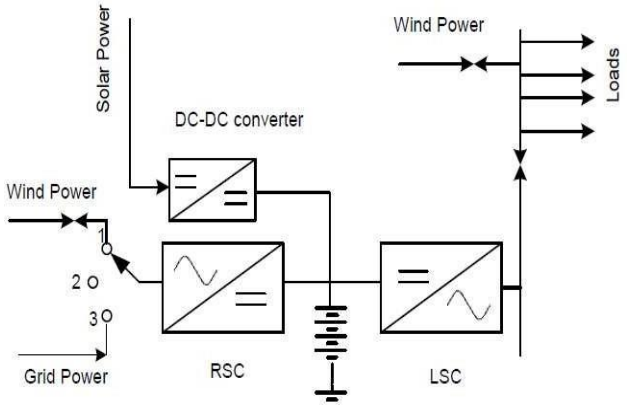

Figure 3: Diagram illustrates the energy flow in a remote micro grid network that uses battery storage to store energy from renewable sources.

Wind turbines give the DFIG drive torque while absorbing the kinetic energy of the wind. RSC meets all of the machine's magnetization force requirements when the wind turbine is running. Therefore, a 15kW wind turbine's mechanical power can be converted into electrical energy using just 11.83 kW of DFIG power. A zigzag transformer connects the load and stator terminals to the LSC, providing neutral for single-phase loads on the 415V side as well. The maximum rotor voltage Vmax is 125 V (0.3 x 415 V), which is equal to the maximum absolute value of the rotor slip, which is 0.3.

It is also decided that the voltage on the LV side of the zigzag transformer will be equal to Vmax. As a result, the transformer's voltage ratio is 415/125 V, and the stator and load are linked to its HV winding.

The whole kVA demand for the load and the attached filter must be satisfied by the zigzag transformer. Consequently, a 20 kVA transformer is chosen. In addition to fulfilling the disabled power need of the linked load and filter during peak demand, this is sufficient to transfer the rated power. Banks of lead-acid batteries can run risk-free between 2.25V and 1.8V per cell. This leads to a battery voltage Vb max maximum and Vb min minimum of 270V and 216V, respectively. The battery bank is considered to have a fictitious capacitor Cb, an internal resistance Rin, and a DC power source linked in series. Another resistor Rb is also attached to the battery's ends to show how much energy is used during the battery's self-discharge. The solar cell is the fundamental component of a solar PV system. a solar converter that uses SMPPT logic and a boosted DCDC converter for solar energy evacuation. The gradual conductivity method serves as its foundation. SMPPT manipulates us by cleverly altering how MPP interacts

with our solar system. Since onshore wind turbines only produce energy for about 70% of the time, the system must be built to function even when there is no wind.

comparable to the control diagram in the illustration. 4.3, i*qs is made up of two parts.

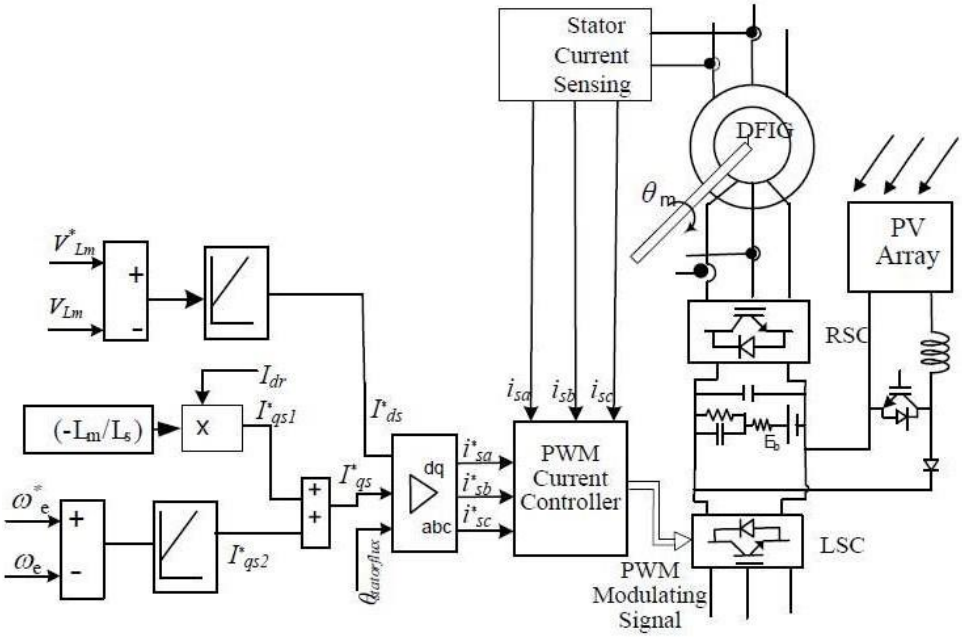

Figure 4: LSC control schematic for a micro grid powered by REGS

The stator frequency is controlled by the LSC. The system needs to generate a nominal frequency, but it has built-in drooping characteristics. Vdc max is assumed to be 272.5V. This is the bus voltage corresponding to Vb max during charging. Similarly, Vdc min is assumed to be 213.5V, this bus voltage corresponds to Vb min and the battery is discharged. Using these numbers, the frequency will vary from 49Hz to 51Hz. The RSC regulates the speed

of the turbine so that the system operates in MPP regardless of changes in wind conditions. It also supplies magnetization force to the generator. As shown in Figure 4, the control philosophy includes control algorithms for determining the orthogonal component of the rotor current and the DC components.

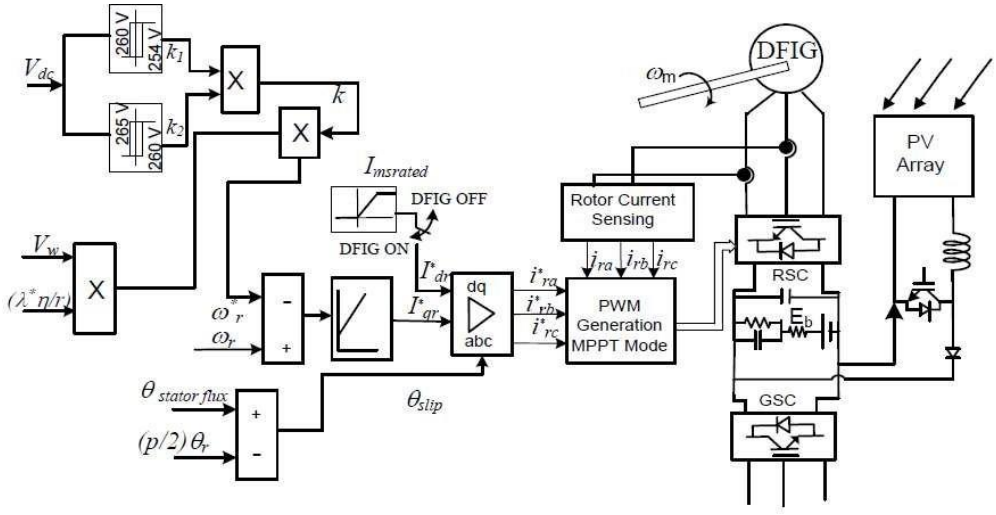

Figure 5: RSC control schematic for a micro grid fed by REGS

Figure 4 illustrates how two relays, k1 and k2, determine the value of k. The output of the relay falls to 0.85 when the voltage in the intermediate circuit surpasses the threshold. Both relays' thresholds are maintained at 260 and 265 respectively. K achieves values of 0.85 and 0.72 when Vdc crosses 260V and 265V, respectively. Stability current controller produces an RSC control signal from

reference current and detection current (ira, irb, and irc) error signals.

IV. SIMULATION RESULTS

The Mat lab is used to create the Simulink model of the micro-grid powered by REGS. The functionalities of the wind turbine and solar panels are modelled.

CASE-A: Performance of System under Constant Load and Wind Power Input and Output

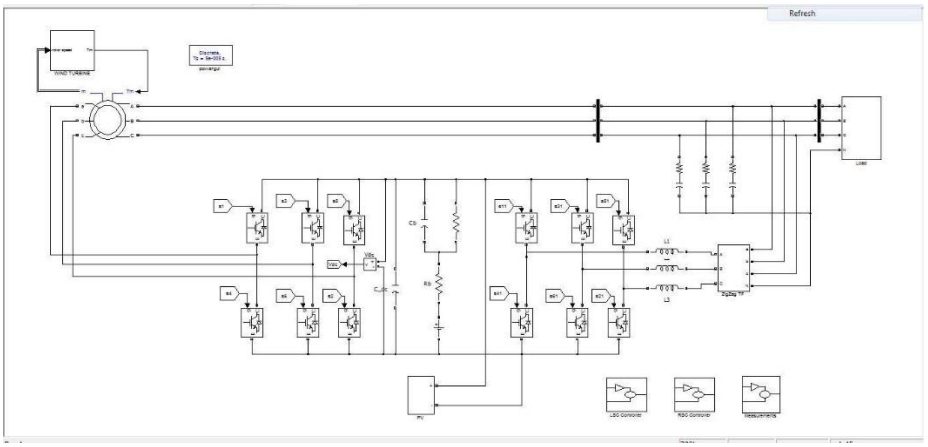

Figure 6: System Performance at Constant Load and Wind Power Cut-in and Cut-out

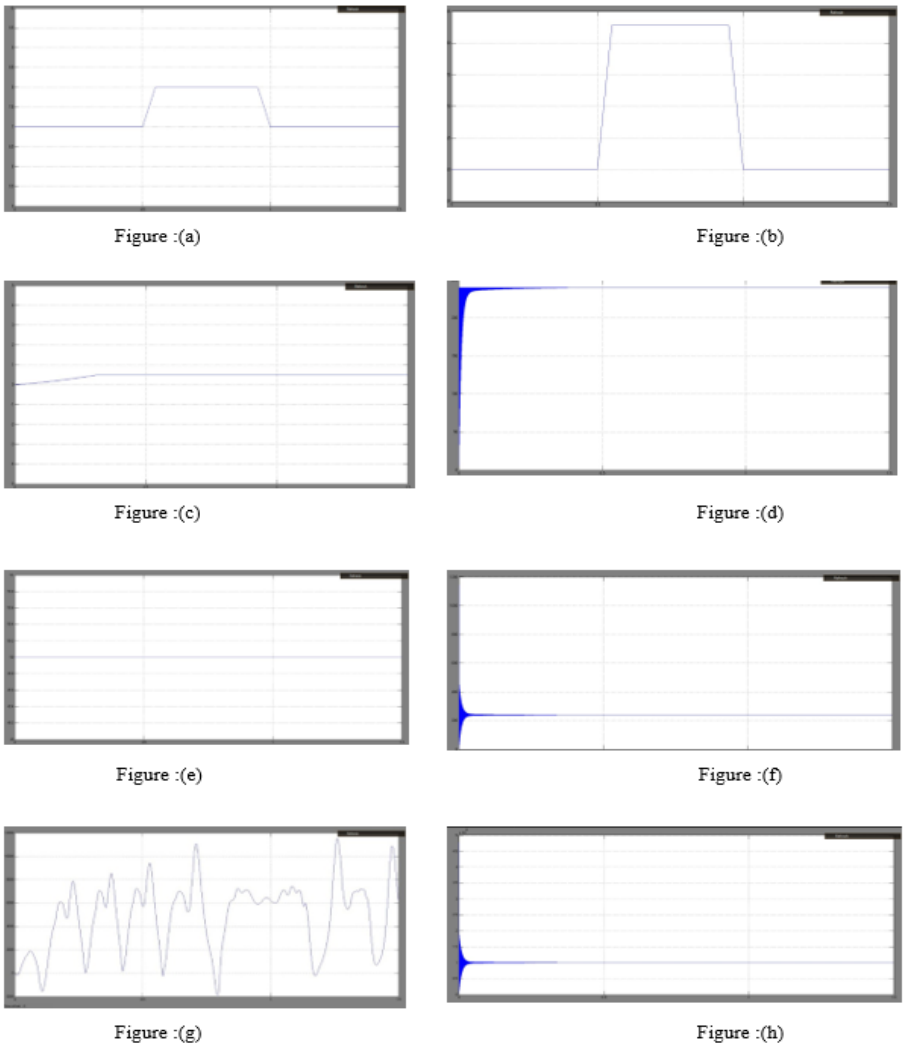

Figure :(a) Figure :(b)

Figure :(c) Figure :(d)

Figure :(e) Figure :(f)

Figure :(g) Figure :(h)

Figure 7: Performance of a micro grid powered by wind and fed by REGS

Without using wind or solar energy, the system boots up with a load of 10kW and 6kVAR, as illustrated in Figure 7. The wind turbine is operational at a wind speed of 7 m/s at t = 0.25 s. Momentary changes in system voltage are as a result seen. The wind speed at the turbine increases from 7 m/s to 8 m/s at t = 0.6 s, then returns to its initial value at t = 0.1 s. According to the WMPPT algorithm, the rotor control operation maintains the desired rotational speed. The wind turbine will turn off when t = 0.14 seconds.

CASE-B: Performance of System under Constant Load and Solar Power Input and Output

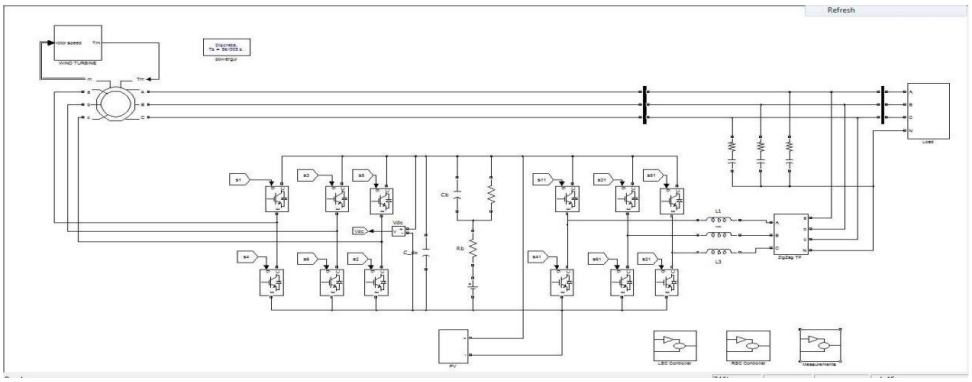

Figure 8: System performance under constant load and with solar power turned on and off

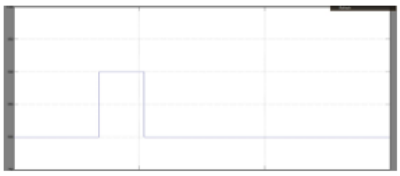

Figure: (a)

Figure: (b)

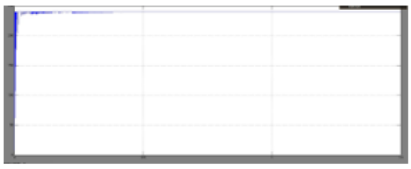

Figure: (c)

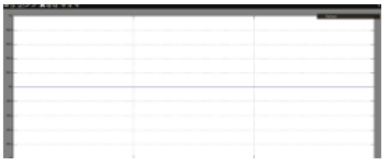

Figure: (d)

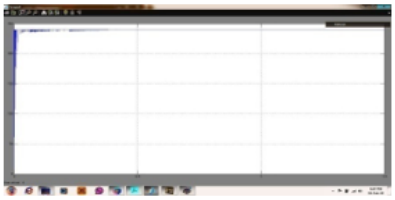

Figure: (e)

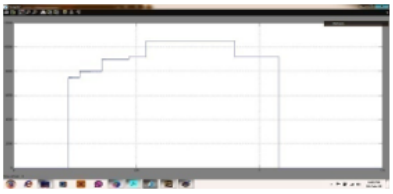

Figure: (f)

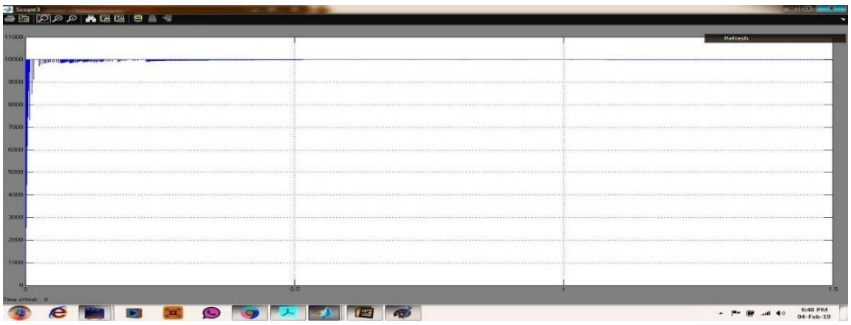

Figure 9: The system's performance without a power supply and a solar power system is put into use.

Without using wind or solar energy, the system is launched with 10 kW and 6 KVAR loads. As seen in Fig. 9, the solar system begins to function at t = 0.25 s with radiation of 800 W/m2. The sun irradiance rises to 900 W/m2 at t = 0.4 s and then falls back to 800 W/m2 at t = 0.6 s. The solar converter operates at SMPPT and controls the solar PV voltage. The solar system shuts off at time t = 0.7 s. At any of the transition points, there were no appreciable changes in the system voltage. CASE-C: Performance of System at Unbalanced Nonlinear Load

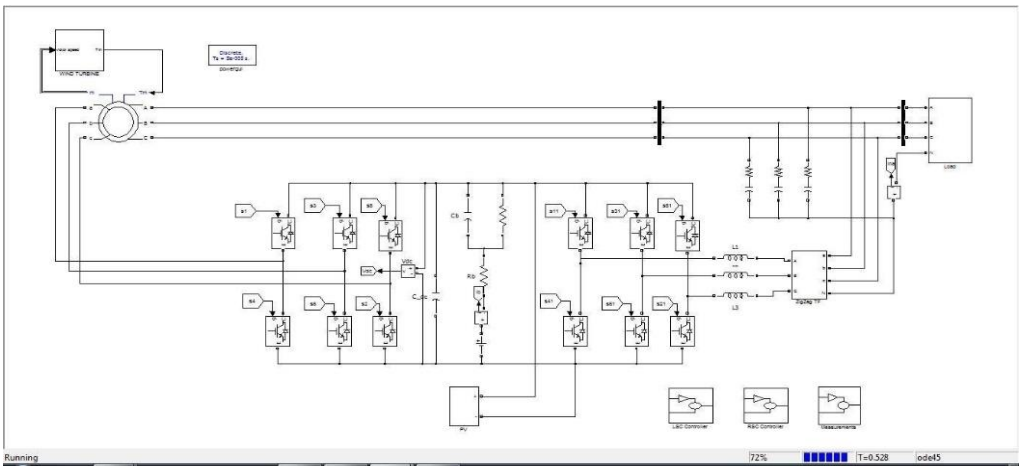

Figure 10: System Performance under Unbalanced Nonlinear Load

Figure: (a)

Figure: (b)

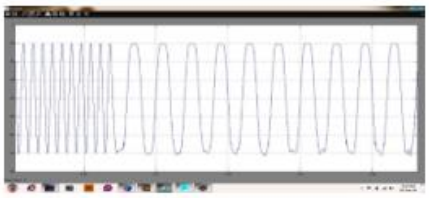

Figure: (c)

Figure: (d)

Figure: (e)

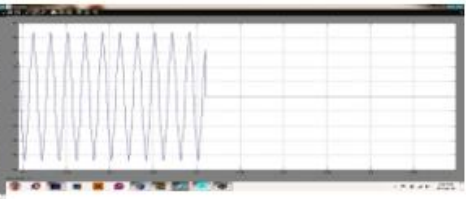

Figure: (f)

Figure: (g)

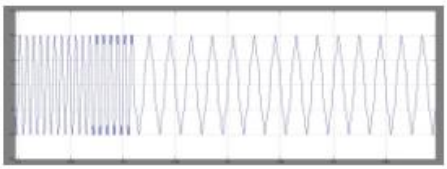

Figure: (h)

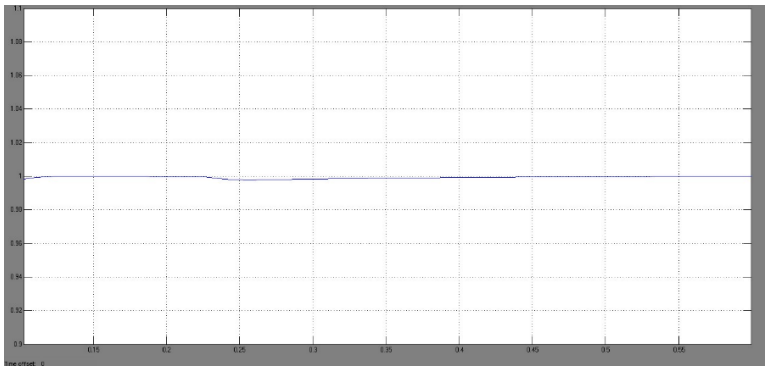

Figure 11: System performance under an imbalanced, nonlinear load

The performance of a system with imbalanced non-linearity is depicted in Figure 10 and 116. The unbalanced nonlinear load requirements must be met by the micro grid. The worst case scenario is presummated if there is no source. A 2kW linear load plus an 8kW non-linear load make up the connection load. The a-phase load is disconnected from the grid at t = 0.325s, and the b-phase load is detached from the grid at t = 0.346s. The findings demonstrate that the system is capable of offering clients with both unbalanced and non-linear loads high-quality performance.

CASE-D: Performance of System at Loss of Load

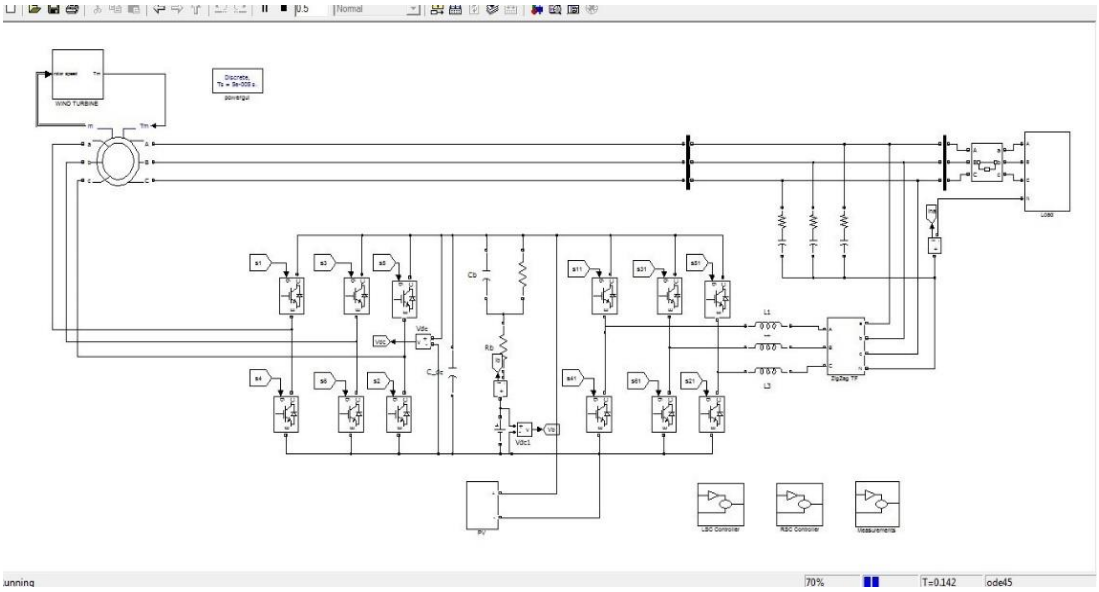

Figure 12: System Performance During Load Loss

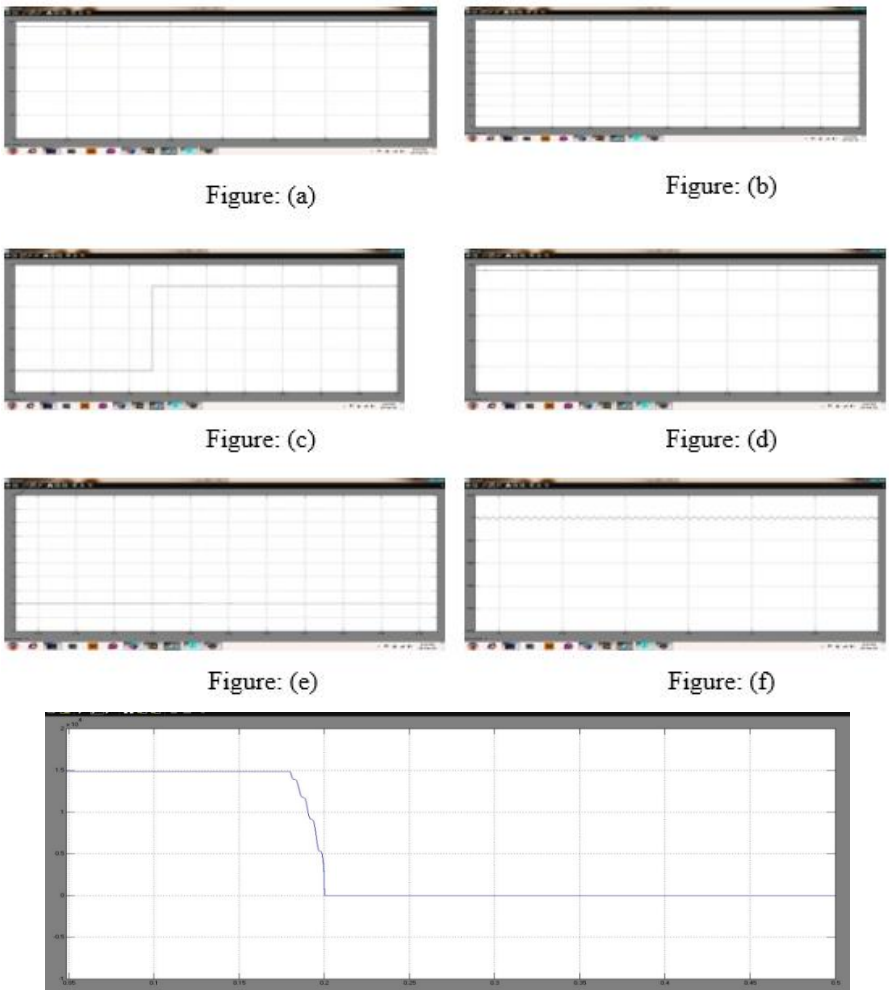

Figure 13: System performance at battery power when the load is lost

10kW and 6KVAR loads are attached to the terminals before the simulation begins. The load is powered by batteries because there is no access to wind or solar energy. The system load is disabled when t = 0.2 seconds. As you can see, the network's frequency and system voltage stay consistent.

CASE-E: System Running without Generating Source and Battery Charged from the- grid

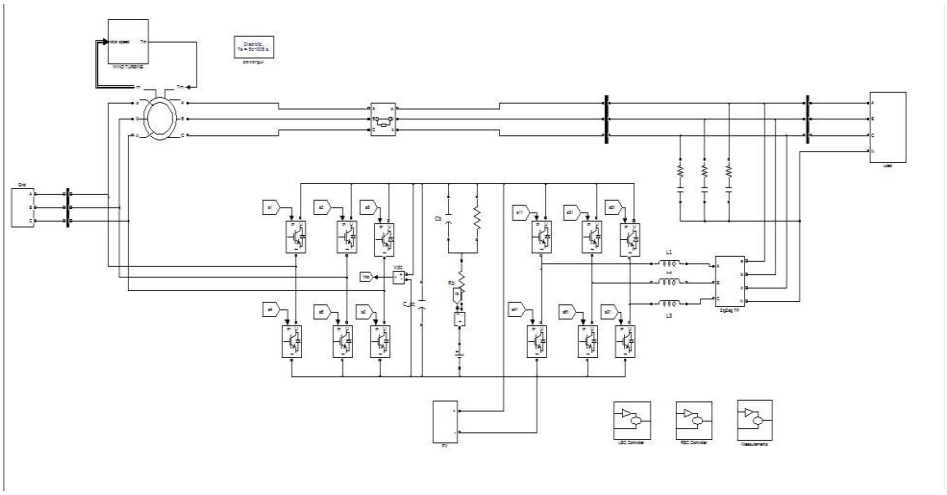

Figure 14: System Running without Generating Source and Battery Charged from the Grid

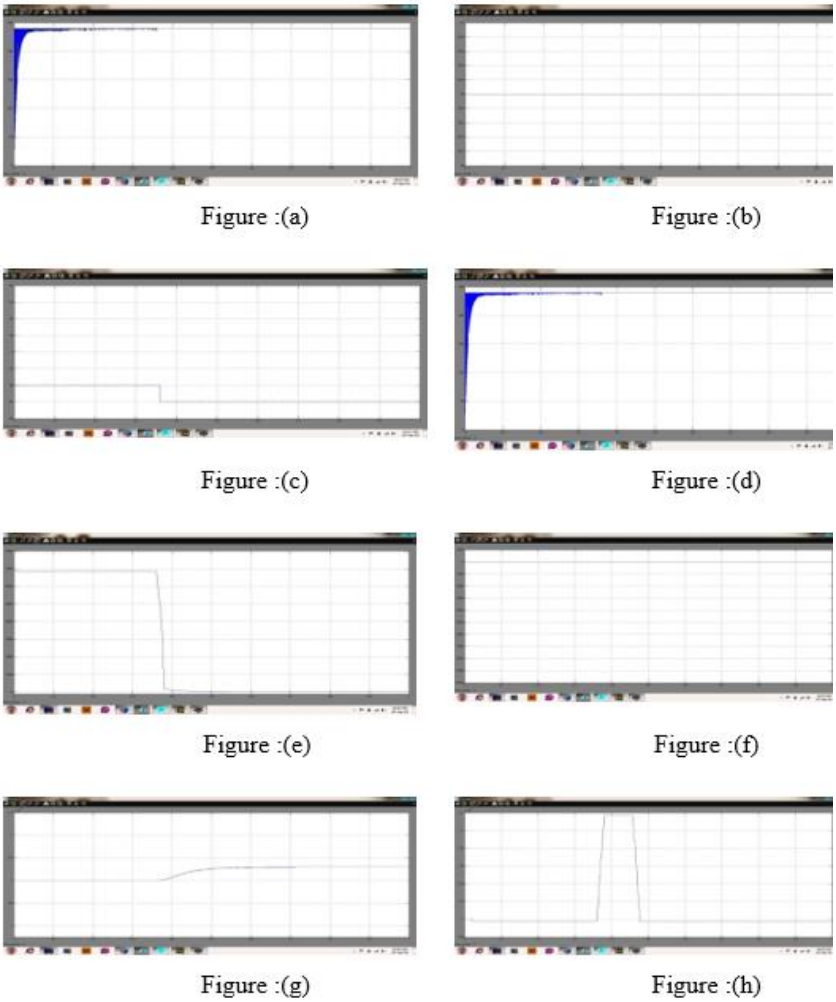

Figure 15: system performance with external charging

Figures depicts a situation in which there is no electricity to the grid and a depleted battery. To keep the load requirement constant, an external load is needed. In accordance with the logic situation, the charging circuit is turned on. The wind generation stops at t = 0.4 s, and the charging circuit kicks in as a result of the battery voltage dropping. So, in addition to charging the battery, external power is fed through the RSC to meet the needs for charging.

CASE-F. System performance under high generation and DC bus overvoltage scenarios

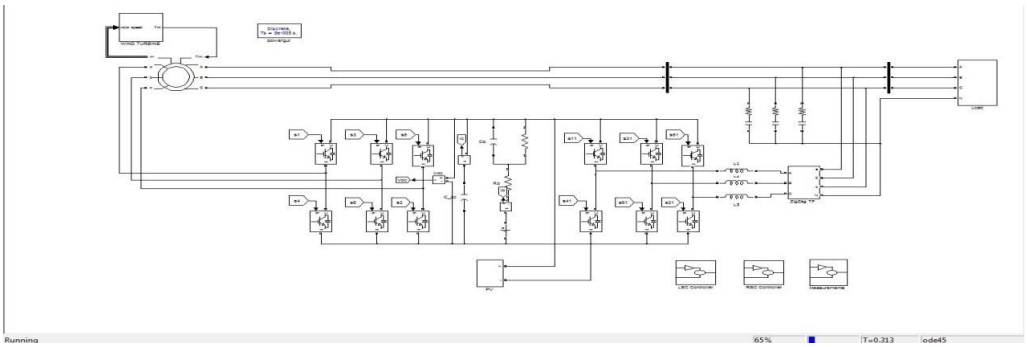

Figure 16: System Performance under High Generation and Over-voltage DC Bus Scenario

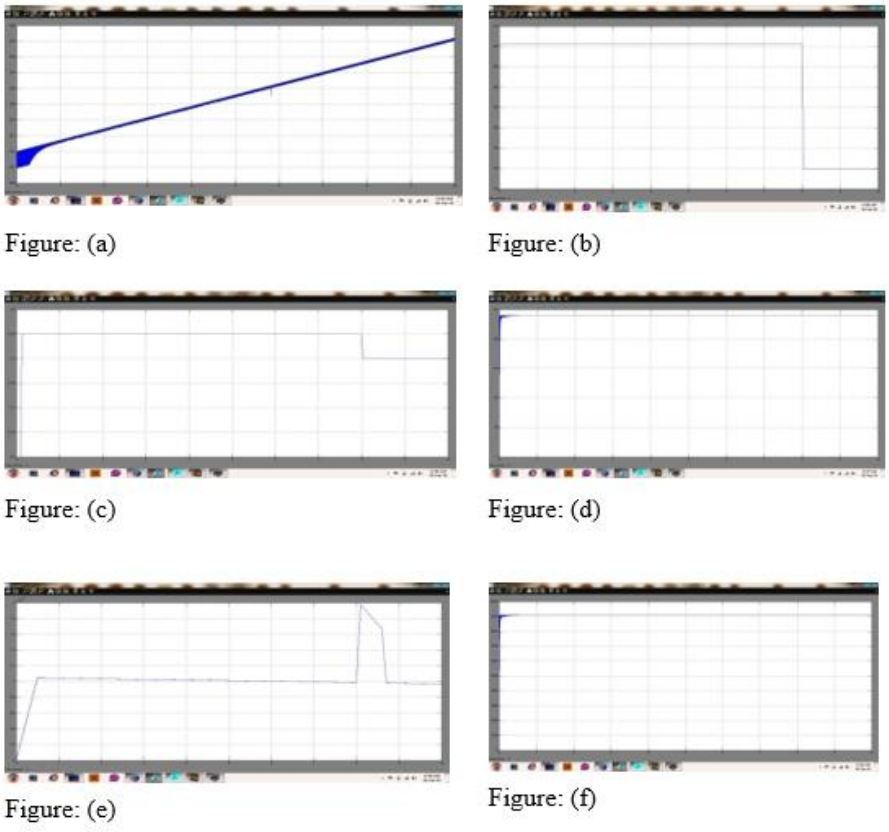

Figure 17: System performance in conditions of high generation and DC bus overvoltage

Figure 16 and 17 illustrates the machine's performance during extreme internet usage and a DC bus overvoltage condition. The AH of the battery is reduced by utilising 1/200 times in order to make the effect noticeable. Saved are nine metres per second (m/s) of wind speed and 700 W/m2 of solar radiation, respectively. The curve clearly shows that the RSC manipulator lowers the DFIG pace set factor to 85% of the MPPT set factor when the Vdc reaches 260 V. From Fig. 12, it is clear that the charging power, Pc, and voltage upward thrust have all decreased.

V. CONCLUSION

A rural site with few residents is determined to be able to meet its charging needs using the planned REGS power supply microgrid system. In order to get the most energy from renewable energy sources while still giving users high-quality electricity, REGS is made up of wind and solar energy blocks. The system is set up to run entirely autonomously. The determination of the primary component's dimensions is also covered in this study.

Performance of the system has been demonstrated for various input conditions for various load configurations. The power quality at the charging terminals is consistently within acceptable bounds. The outcomes of laboratory experiments using prototypes show the system's effectiveness as well. The system also takes outside factors into.

CONFLICTS OF INTEREST

The authors declare that they have no conflicts of interest.

REFERENCES

[1] H. Zhu, D. Zhang, H. S. Athab, B. Wu and Y. Gu, "PV Isolated Three- Port Converter and Energy-Balancing Control Method for PV-Battery Power Supply Applications," IEEE Transactions on Industrial Electronics, vol. 62, no. 6, pp. 3595-3606, June 2015.

[2] M. Das and V. Agarwal, "Novel High-Performance Stand-Alone Solar PV System with High-Gain High-Efficiency DC–DC Converter Power Stages," IEEE Transactions on Industry Applications, vol. 51, no. 6, pp. 4718-4728, Nov.-Dec. 2015.

[3] A. B. Ataji, Y. Miura, T. Isa and H. Tanaka, "Direct Voltage Control with Slip Angle Estimation to Extend the Range of Supported Asymmetric Loads for Stand-Alone DFIG," IEEE Transactions on Power Electronics, vol. 31, no. 2, pp. 1015-1025, Feb. 2016.

[4] N.A. Orlando, M. Liserre, R.A. Mastromauro and A. Dell 'Aquila, "A survey of control issues in PMSG-based small wind turbine system," IEEE Trans. Industrial Informatics, vol.9, no.3, pp 1211-1221, July 2013.

[5] T. Hirose and H. Matsuo, "Standalone Hybrid Wind-Solar Power Generation System Applying Dump Power Control Without Dump Load," IEEE Trans. Industrial Electronics, vol. 59, no. 2, pp. 988-997, Feb. 2012.

[6] Z. Qi, "Coordinated Control for Independent Wind-Solar Hybrid Power System," 2012 Asia-Pacific Power and Energy Engineering Conference, Shanghai, 2012, pp. 1-4.

[7] M. Rezkallah, S. Sharma, A. Chandra and B. Singh, "Implementation and control of small- scale hybrid standalone power generation system employing wind and solar energy," 2016 IEEE Industry Applications Society Annual Meeting, Portland, OR, 2016, pp. 1-7.

[8] A. Hamadi, S. Rahmani, K. Addoweesh and K. Al-Haddad, "A modeling and control of DFIG wind and PV solar energy source generation feeding four wire isolated load," IECON 2013 - 39th Annual Conference of the IEEE Industrial Electronics Society, Vienna, 2013, pp. 7778-7783.

[9] S. K. Tiwari, B. Singh and P. K. Goel, "Design and control of autonomous wind-solar energy system with DFIG feeding 3-phase 4-wire network," 2015 Annual IEEE India Conference (INDICON), New Delhi, 2015, pp. 1-6.

[10] S. K. Tiwari, B. Singh and P. K. Goel, "Design and control of micro-grid fed by renewable energy generating sources," 2016 IEEE 6th Inter. Conference on Power Systems (ICPS), New Delhi, 2016, pp. 1-6.

[11] H. Polinder, F. F. A. van der Pijl, G. J. de Vilder and P. Tavner, "Comparison of direct- drive and geared generator concepts for wind turbines," IEEE International Conference on Electric Machines and Drives, 2005., San Antonio, TX, 2005, pp. 543-550.

[12] Emmanouil A. Bakirtzis and Charis Demoulias "Control of a micro-grid supplied by renewable energy sources and storage batteries," XXth Inter. Conf. on Electrical Machines (ICEM), pp. 2053-2059, 2-5 Sept. 2012.

[13] S. Heier, Grid Integration of Wind Energy Conversion Systems. Hoboken,NJ: Wiley, 1998.

[14] Z.M. Salameh, M.A. Casacca and W.A. Lynch, "A mathematical model for lead-acid batteries," IEEE Trans. Energy Convers., vol. 7, no. 1, pp. 93-97, Mar.1992.

[15] A B. Rey-Boué, R García-Valverde, F de A. Ruz-Vila and José M. Torrelo-Ponce, "An integrative approach to the design methodology for 3-phase power conditioners in Photovoltaic Grid-Connected systems," Energy Conversion and Management, vol. 56, pp. 80–95, Dec 2011.

[16] Z Xuesong,Song Daichun,Ma Youjie and Cheng Deshu, "The simulation and design for MPPT of PV system based on incremental conductance method," 2010 WASE Inter. Conf. on Information Engineering, Aug, 2010, pp.314 – 317.

[17] Shailendra. Kr. Tiwari, B. Singh and P. K. Goel, "Design and Control of Autonomous Wind-Solar Hybrid System with DFIG Feeding a 3-Phase 4-Wire System," in IEEE Transactions on Industry Applications, vol. PP, no. 99, pp. 1-1.

[18] S. Kumar Tiwari, B. Singh and P. K. Goel, "Design and Control of Microgrid Fed by Renewable Energy Generating Sources," in IEEE Transactions on Industry Applications, vol. 54, no. 3, pp. 2041-2050, May-June 2018, doi: 10.1109/TIA.2018.2793213.

[19] [19] S. Kumar Tiwari, B. Singh and P. K. Goel, "Design and Control of Microgrid Fed by Renewable Energy Generating Sources," in IEEE Transactions on Industry Applications, vol. 54, no. 3, pp. 2041-2050, May-June 2018, doi: 10.1109/TIA.2018.2793213.

[20] Rezkallah, M. & Singh, Sanjeev & Chandra, Ambrish & Singh, Bhim & Tremblay, Marco & Saad, M. & Geng, Hua. (2019). Comprehensive Controller Implementation for Wind-PV-Diesel Based Standalone Microgrid. IEEE Transactions on Industry Applications. PP. 1-1. 10.1109/TIA.2019.2928254.

[21] file:///C:/Users/PACE%20-%20EEE/Downloads/43663.pdf

[22] https://nehu.ac.in/public/uploads/Annual_Report_2019.pdf

[23] Hanna Mäkinen, Janne Kaseva, Perttu Virkajärvi, Helena Kahiluoto, shifts in soil–climate combination deserve attention, Agricultural and Forest Meteorology, Volumes 234–235, 2017, Pages 236-246, ISSN 0168-1923,